SWOT-JAXA: Japanese oceanographic research in SWOT

Development of calibration/validation and assimilation methods of wide-swath sea surface height measurements in the western North Pacific and surrounding marginal seas

PI: Kai MATSUI (JAXA),
*Osamu ISOGUICHI(RESTEC), Kaoru ICHIKAWA(Kyushu University), Yasumasa MIYAZAWA(JAMSTEC), Naoki Hirose (Kyushu University)

1. New cal/val methods for SWOT snapshot SSH field – Ichikawa et al. (2019)

- Low-cost GNSS reflectometry (GNSS-R) altimetry on an unmanned aerial vehicle (UAV) was examined by mounting LHCP and RHCP antennas and two classical GNSS receivers on a UAV.
- To obtain the sea surface height (**Hs**), the vertical distance of the reciever antenna from the sea surface (**h**) was separately determined together with the GNSS antenna height (**Ha**). The **h** can be determined by measuring the excess path length of the reflected GNSS signals with respect to the direct signals (Fig.1-1)
- In order to effectively receive the reflected signals, an LHCP antenna (Antcom 4G15L-A-XS-1) was used as the downward antenna (Fig. 1-2(b)), while an RHCP antenna (Tallysman TW4721) was selected for the upward antenna (Fig. 1-2(a)).
- The height of UAV (**Ha**) was determined by the RTKLIB post-processed kinematic (PPK) positioning method by referring to our base station, which is critical in high precision measurement .

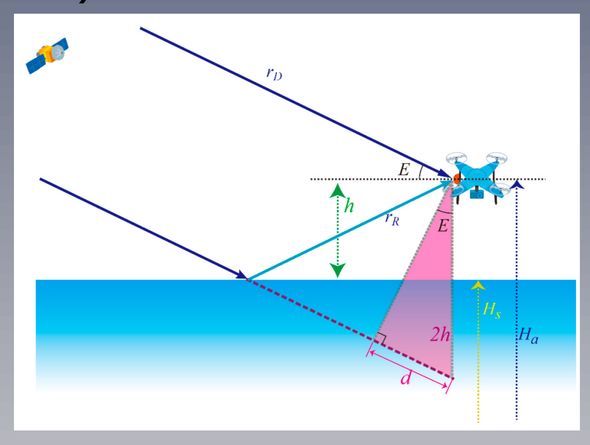

Fig. 1-1. Schematic figure of GNSS-R altimetry on a UAV.

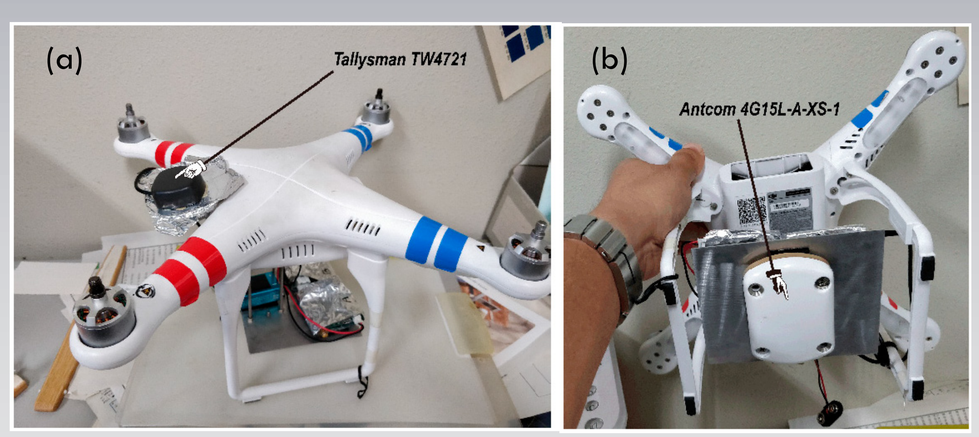

Fig. 1-2. The GNSS-R altimeter use in the experiments: (a) Top view; (b) Bottom view. d

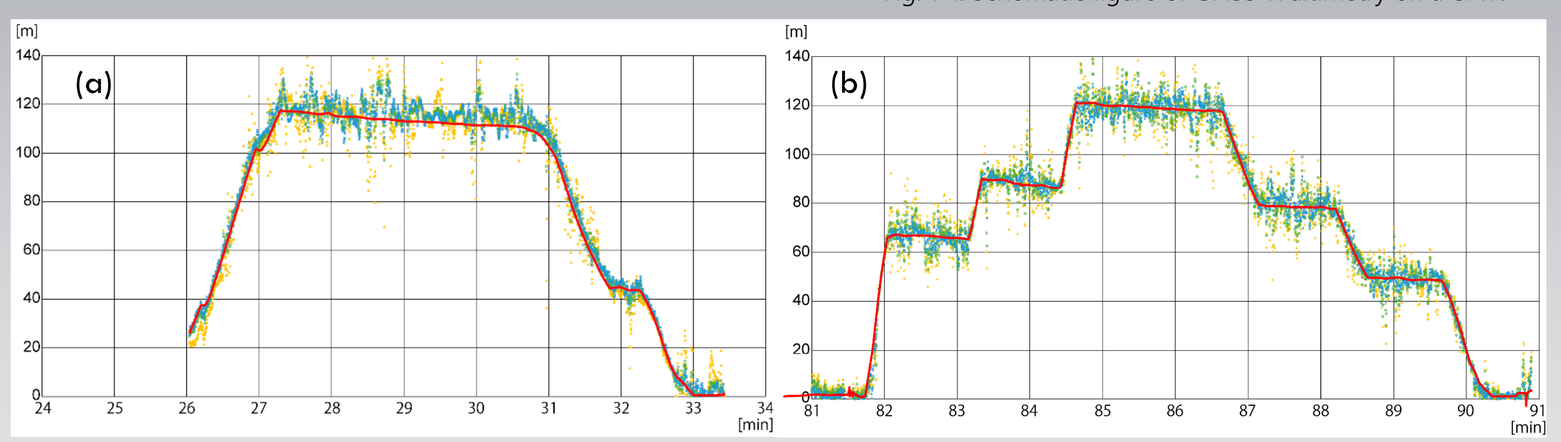

Fig. 1-3. Time series of the measured altitude of the UAV, **H** (red curve), and the estimated heights **h** with various weight functions in (a) the first and (b) the second experiments; blue crosses for w_{no}(=1), green circles for w_s(=sin(E)), and yellow triangles for w_{st}(=sin(E)tan(E)). The abscissa is the elapsed time in minutes from noon on 7 January 2017 (local JST).

Result

- In the present study, the vertical distance from the sea surface (**h**) were compared instead of **Hs**. Using the water-level height (**Hs**) at the closest water level observatory, and the measured altitude of the UAV (**Ha**), the measured altitude of the UAV from the water level (**H**= **Ha** - **Hs**) was calculated to compare with the height estimated by the GNSS-R method (**h**) (Fig.1-3).
- In general, the measured ascending , hovering, and descending statuses of the UAV were well represented in the estimated altitudes.
- When comparing the first and second flights, it can be seen that the GNSS-R altimetry performed better in the second flight since the elevation angles of the GPS satellites were generally higher in the second flight.
- In the better-quality second flight, the mean discrepancy between the measured and estimated heights archives an accuracy of the order of 0.01 m, which is well compatible with that of the 5 Hz PPK positioning of the UAV height (**Ha**).
- Note that a large number of UAVs can be constellated because of the low-cost nature of the present method, which would enable the provision of water level maps with high resolution and wide coverage that could be used to validate wide-swath altimeters, such as SWOT.

Reference

Ichikawa et al. (2019), Low-Cost GNSS-R Altimetry on a UAV for Water-Level Measurements at Arbitrary Times and Locations, *Sensors* **2019**, 19, 998; doi:10.3390/s19050998.
Gaultier, L., C. Ubelmann, and L.-L. Fu, (2016): The Challenge of Using Future SWOT Data for Oceanic Field Reconstruction. J. Atmos. Oceanic Technol., 33, 119-126, doi:10.1175/jtech-d-15-0160.1.

2. Data Assimilation for SWOT data

- JAXA launched a "coastal forecast core team" with the cooperation of the Operational Oceanographic Organization of Japan, and is examining the future use of the wide-swath-type altimeter. As part of that activity, observing system simulation experiment (OSSE) using SWOT simulation data that were produced by the SWOT simulator (Gaultier et al. (2016)) is being conducted.
- Table 2-1 represents model specifications used for two types of OSSEs and Fig.2-1 shows the examples of the SWOT simulated data for sbPOM.
- Table 2-2 and 2-3 show model equations and basic parameters of the 2D shallow-water model. **Nature Run (NR)** is forced by NAO.99 (Matsumoto et al., 2000) tide model with bottom topography of J-TOPO1 with some corrections and substitutions (Hirose 2005), while **Extended Run (ER)** are forced by Oregon state university Tide Prediction Software(OTPS) with bathymetry of assemblage of NGDC, SIO, LDEO data (Smith and Sandwell, 1997).
- Figs. 2-2 and 2-3 show preparation of experiment: topography difference map and comparisons of sea levels between **NR** and **ER**.

Table 2-1. Model specifications used by OSSE.

Institution	Model	Area	Grid	Assimilation method	Boundary condition	Atmo. Forcing	Remarks
JAMSTEC	sbPOM	128°-148°E 28°-48°N	1/36°	3DVAR (4DEnVAR)	JCOPE2M	NCEP/NCAR RA1	
Kyushu Univ.	2D shallow-water model	East China Sea Japan Sea	1/12°×1/15°	None	Matsumoto et al. (2000)	Boundary condition	Tide evaluation with barotropic model

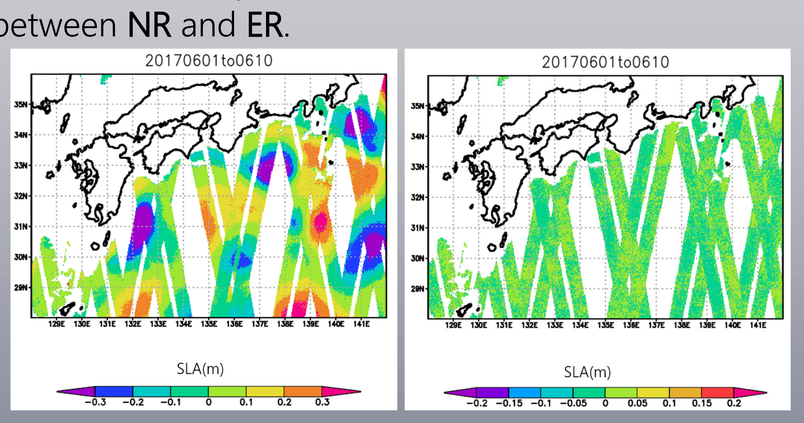

Fig 2-1. Example of SWOT simulated data for 7days from 1st June 2017 to 10th June 2017: (a) model SLA, and (b) Karin Noise.

Table 2-2. Model equations. Shallow water model (Y.ONUKI 2017), using potential enstrophy and energy conserving scheme in Arakawa C-grid (Arakawa & Lamb 1981)

$$\frac{\partial \eta}{\partial t}+\frac{1}{a\cos\phi}\frac{\partial}{\partial\lambda}(uH)+\frac{1}{a\cos\phi}\frac{\partial}{\partial\phi}(vH\cos\phi)=0$$

$$\frac{\partial u}{\partial t}+\frac{u}{a\cos\phi}\frac{\partial u}{\partial\lambda}+\frac{v}{a}\frac{\partial u}{\partial\phi}-\frac{uv}{a}\tan\phi-fv=-\frac{g}{a\cos\phi}\frac{\partial\eta}{\partial\lambda}-ru\frac{\sqrt{u^2+v^2}}{H}+A_h\{\nabla^2u-\frac{1+\tan^2\phi}{a^2}u-\frac{2\sin\phi}{a^2\cos^2\phi}\frac{\partial v}{\partial\lambda}\}$$

$$\frac{\partial v}{\partial t}+\frac{u}{a\cos\phi}\frac{\partial v}{\partial\lambda}+\frac{v}{a}\frac{\partial v}{\partial\phi}+\frac{u^2}{a}\tan\phi+fu=-\frac{g}{a}\frac{\partial\eta}{\partial\phi}-rv\frac{\sqrt{u^2+v^2}}{H}+A_h\{\nabla^2v-\frac{1+\tan^2\phi}{a^2}v+\frac{2\sin\phi}{a^2\cos^2\phi}\frac{\partial u}{\partial\lambda}\}$$

t : Time
η : Sea Level
u : Longitudinal Velocity
v : Latitudinal Velocity
H : Depth
λ : Longitude
f : Coriolis Parameter
A_h: Viscosity
g: Standard Gravity
r : Drag of Bottom
a : Earth Radius
ϕ : Latitude

Table 2-3. Model parameters.

	Parameters
Resolution	1/12°(lon) × 1/15°((Lat)
Bottom drag (r)	2.7×10^{-3}
Viscosity(A_h)	1×10^2 m^{2}s^{-1}
Standard Gravity(g)	9.81 m s^{-2}
Initiate date	2017/1/1
Duration	50days
Tide force nudging	60^{-1} s^{-1}
Main Tide Constituents	M2, P1,S2, K1,O1,N2, Q1,K2

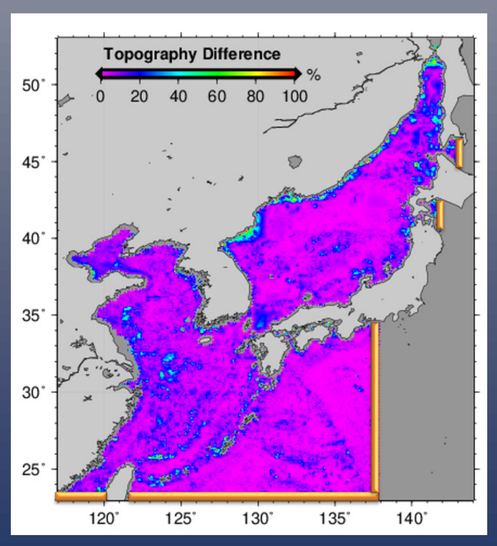

Fig 2-2. Model domain and topography difference between NR and ER. Orange show tide force area.

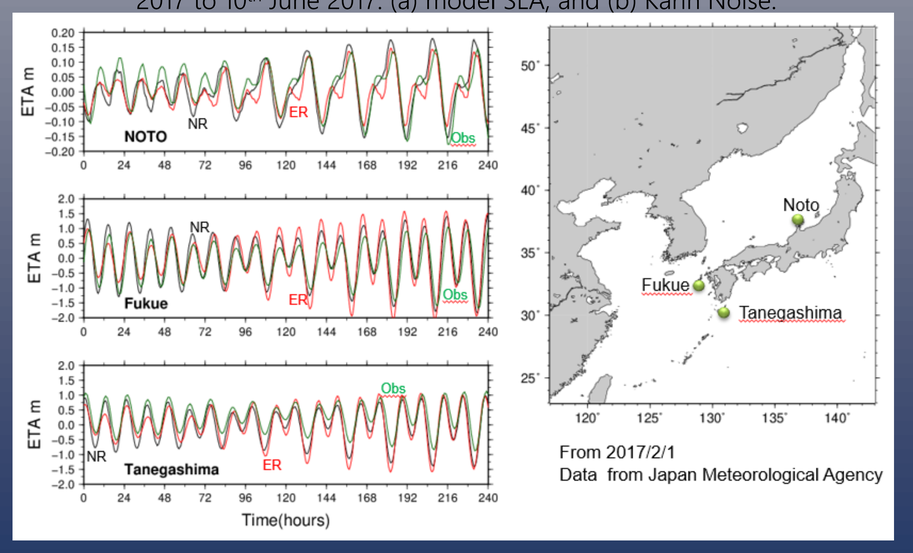

Fig 2-3. Comparison of sea levels from NR (black), ER (red), and observation (green) at 3 tide stations.